

# An Oligosilsesquioxane Cage Functionalized with Molybdenum(II) Organometallic Fragments

Newton L. Dias Filho,<sup>†</sup> Fátima C. M. Portugal,<sup>‡,§</sup> J. M. F. Nogueira,<sup>‡,§</sup> Paula Brandão,<sup>||</sup> Vitor Félix,<sup>||,⊥</sup> Pedro D. Vaz,<sup>‡,§</sup> Carla D. Nunes,<sup>‡,§</sup> Luis F. Veiros,<sup>#</sup> Maria J. Villa de Brito,<sup>‡,#</sup> and Maria José Calhorda<sup>\*,‡,§</sup>

<sup>†</sup>Faculdade de Engenharia de Ilha Solteira, UNESP-Univ Estadual Paulista, Departamento de Física e Química, Av. Brasil Centro, 56 CEP 15385-000, Ilha Solteira SP, Brasil

<sup>‡</sup>Universidade de Lisboa, Faculdade de Ciências, Departamento de Química e Bioquímica, Campo Grande, 1749-016 Lisboa, Portugal

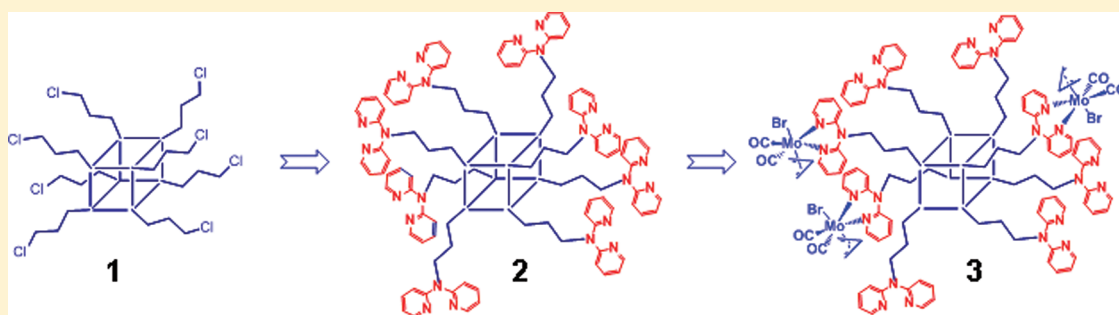
<sup>§</sup>Universidade de Lisboa, Faculdade de Ciências, Centro de Química e Bioquímica, Campo Grande, 1749-016 Lisboa, Portugal

<sup>||</sup>Departamento de Química, Universidade de Aveiro, CICECO, 3810-193 Aveiro, Portugal

<sup>⊥</sup>Secção Autónoma de Ciências da Saúde, Universidade de Aveiro, 3810-193 Aveiro, Portugal

<sup>#</sup>Centro de Química Estrutural, Instituto Superior Técnico, Universidade Técnica de Lisboa, Av. Rovisco Pais 1, 1049-001 Lisboa, Portugal

## Supporting Information



**ABSTRACT:** A silsesquioxane cage polymer functionalized with eight chloropropyl arms (**1**, T<sub>8</sub>-PrCl) reacted with 2,2'-dipyridylamine (DPA) to afford a new derivative with eight pendant linear chains (**2**, T<sub>8</sub>-Pr-DPA). Further reaction with [Mo( $\eta^3$ -C<sub>3</sub>H<sub>5</sub>)Br(CO)<sub>2</sub>(NCMe)<sub>2</sub>] afforded another derivative containing three molybdenum units (**3**, T<sub>8</sub>-Pr-DPA-Mo), after substitution of the two nitrile ligands in each complex. These are the first silsesquioxane species containing DPA and the Mo( $\eta^3$ -C<sub>3</sub>H<sub>5</sub>)Br(CO)<sub>2</sub> fragment. The three materials were characterized by <sup>1</sup>H, <sup>13</sup>C, <sup>29</sup>Si, and <sup>95</sup>Mo NMR, FTIR, XRD, and elemental analysis, and T<sub>8</sub>-PrCl (**1**) was also structurally characterized by single-crystal X-ray diffraction. It was identified as a low-temperature polymorph of this material. Elemental analysis indicated that all Cl atoms in the parent material T<sub>8</sub>-PrCl (**1**) were substituted by the deprotonated DPA group in T<sub>8</sub>-Pr-DPA (**2**). However, only three [Mo( $\eta^3$ -C<sub>3</sub>H<sub>5</sub>)Br(CO)<sub>2</sub>(DPA)] units were detected in T<sub>8</sub>-Pr-DPA-Mo (**3**). A comprehensive NMR study, complemented with DFT calculations, was carried out in order to detect the effect of Mo coordination on the cage silicon and on the protons and carbons of the propyl chain, but no significant effects were observed. Both <sup>1</sup>H and <sup>29</sup>Si chemical shifts vary upon introducing DPA but remain the same after reaction with the Mo(II) precursor. The <sup>95</sup>Mo NMR data reveal that the metal is not sensitive to the cage. The catalytic activity of **3** was tested as a precursor in the epoxidation of cyclooctene and styrene in the presence of TBHP. Despite the high selectivity toward the epoxides, the conversion and turnover frequencies were low, reflecting the behavior of the [Mo( $\eta^3$ -C<sub>3</sub>H<sub>5</sub>)Br(CO)<sub>2</sub>(DPA)] complex.

## INTRODUCTION

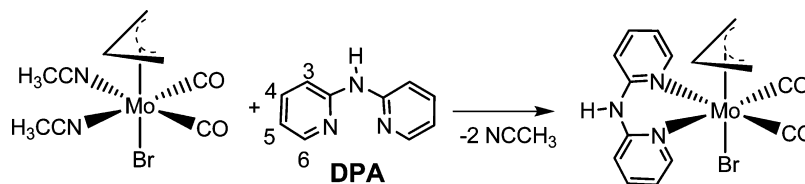
Silsesquioxanes are three-dimensional oligomeric compounds with the general formula (RSiO<sub>1.5</sub>)<sub>2n</sub>, where R can be varied (alkyl, hydrogen, halogen, aryl, etc.). A great number of silicon-based polymers for a wide range of applications have been developed in recent years, and others continue to emerge.<sup>1–3</sup> Among them, polyhedral oligomeric silsesquioxane (POSS) cage molecules, (RSiO<sub>1.5</sub>)<sub>8</sub>, have been attracting a great deal of attention. The (RSiO<sub>1.5</sub>)<sub>8</sub> oligomer consists of a cubic arrangement of Si–O–Si bonds, with the silicon atoms in the

vertices carrying the R groups.<sup>4–6</sup> The size of these particles is in the nanometer range, allowing them to be described as small silica particles. The association with the R substituent gives them a hybrid organic–inorganic character, which can be tuned in order to obtain desirable properties. Functionalization of these particles with catalyst precursors, for instance, leads to new species resembling a catalyst immobilized in normal silica

Received: April 13, 2012

Published: June 13, 2012

Scheme 1



or other support but having the features of a nanomolecule, thereby building a bridge between homogeneous and heterogeneous catalysts. The interest in such approaches has been discussed in one early example addressing the formation of  $[\text{Co}(\text{CO})_4(\text{H}_7\text{Si}_8\text{O}_{12})]$ , with seven hydrogen atoms and one  $\text{Co}(\text{CO})_4$  fragment in the vertices.<sup>7</sup> Soon after, a POSS with two units was obtained and used as a precursor in the formation of new magnetic materials,<sup>8</sup> and the octakis(tetracarbonyl) derivative showed catalytic activity in the hydroformylation of 1-hexene.<sup>9</sup> Other organic groups and metal-containing fragments have similarly been introduced in varying proportions of the vertices.<sup>10</sup>

These and other examples show the variety of patterns for the distribution of R groups. While species with eight R groups are more symmetric<sup>11–15</sup> and might be the model for a “small” heterogeneous catalyst,<sup>16</sup> a POSS with hydrogen atoms and only one functional arm can be considered as a special ligand.<sup>17–20</sup>

The cages may be modified, either by aggregation to form oligomers or even dendrimers or by replacement of one silicon atom by a different one, such as vanadium.<sup>21</sup> The substitution of a Si–R vertex by an M–R group is an alternative way to introduce transition-metal centers in the POSS cage, which usually is carried out during the synthetic procedure, starting from incompletely condensed silsesquioxanes. Metallocene fragments were thus inserted, with the aim of comparing their catalytic properties with those of the unsupported species. Several  $\text{TiR}_2$ <sup>22,23</sup> and  $\text{MCp}_2$  (M = Zr, Hf)-containing silsesquioxanes<sup>24</sup> were synthesized, and their catalytic activity in olefin polymerization has been studied. Zirconium alkoxides were also introduced for epoxidation catalysis.<sup>25</sup> Several computational approaches have been tested to deal with some aspects of transition-metal POSS chemistry.<sup>26–28</sup>

In this work we explore the use of the POSS framework to prepare a polydentate ligand, by functionalizing the cage containing eight chloropropyl pendant arms with the bidentate ligand 2,2'-dipyridylamine (DPA). The reaction between this large ligand and the metal precursor  $[\text{Mo}(\eta^3\text{-C}_3\text{H}_5)\text{Br}(\text{CO})_2(\text{NCMe})_2]$  opens the way to a large molecule, bridging the gap between the homogeneous catalyst  $[\text{Mo}(\eta^3\text{-C}_3\text{H}_5)\text{Br}(\text{CO})_2(\text{DPA})]$  and a classic heterogeneous catalyst where the complex is immobilized in a mesoporous material. The catalytic properties of the final material as a precursor for olefin oxidation were therefore also tested.

## RESULTS AND DISCUSSION

Complex  $[\text{Mo}(\eta^3\text{-C}_3\text{H}_5)\text{Br}(\text{CO})_2(\text{NCCH}_3)_2]$ <sup>29</sup> is a well-known precursor for a wide range of complexes by replacement of the nitriles with other ligands. The choice of ligands can be tuned in order to achieve the desired properties, namely the possibility of reacting with a given functional group using a site different from that used for metal binding. The 2,2'-dipyridylamine ligand (DPA) is a bidentate nitrogen ligand that can

coordinate to Mo to afford a stable complex, bearing at the same time a N–H function able to react further (Scheme 1).<sup>30</sup>

The polyhedral oligomeric silsesquioxane (POSS) cage molecular precursors were prepared by the hydrolysis of 3-chloropropyltriethoxysilane in methanol under acidic conditions.<sup>31</sup> This time-consuming procedure (6 weeks) with a low yield of 35% was recently improved. An alternative synthesis was reported,<sup>32</sup> where the condensation occurs in the presence of di-*n*-butyltin dilaurate as condensation catalyst, reducing the time to only 4 days with an identical yield.

Octakis(3-chloropropyl)octasilsesquioxane (**1**,  $\text{T}_8\text{-PrCl}$ ) reacted with DPA in a molar ratio of 1:8, in the presence of NaH over 22 h, allowing the deprotonated form to perform the nucleophilic substitution at the halogenated carbon atoms of **1**. The coordinating capabilities of the new ligand octakis{3-(2,2'-dipyridylamine)propyl}octasilsesquioxane (**2**,  $\text{T}_8\text{-Pr-DPA}$ ) were then tested by allowing a suspension in ethanol to react with an ethanolic solution of  $[\text{Mo}(\eta^3\text{-C}_3\text{H}_5)\text{Br}(\text{CO})_2(\text{NCMe})_2]$ , under the same conditions as reported for the synthesis in Scheme 1.<sup>30</sup> After workup, a yellow solid containing molybdenum was obtained (**3**,  $\text{T}_8\text{-Pr-DPA-Mo}$ ).

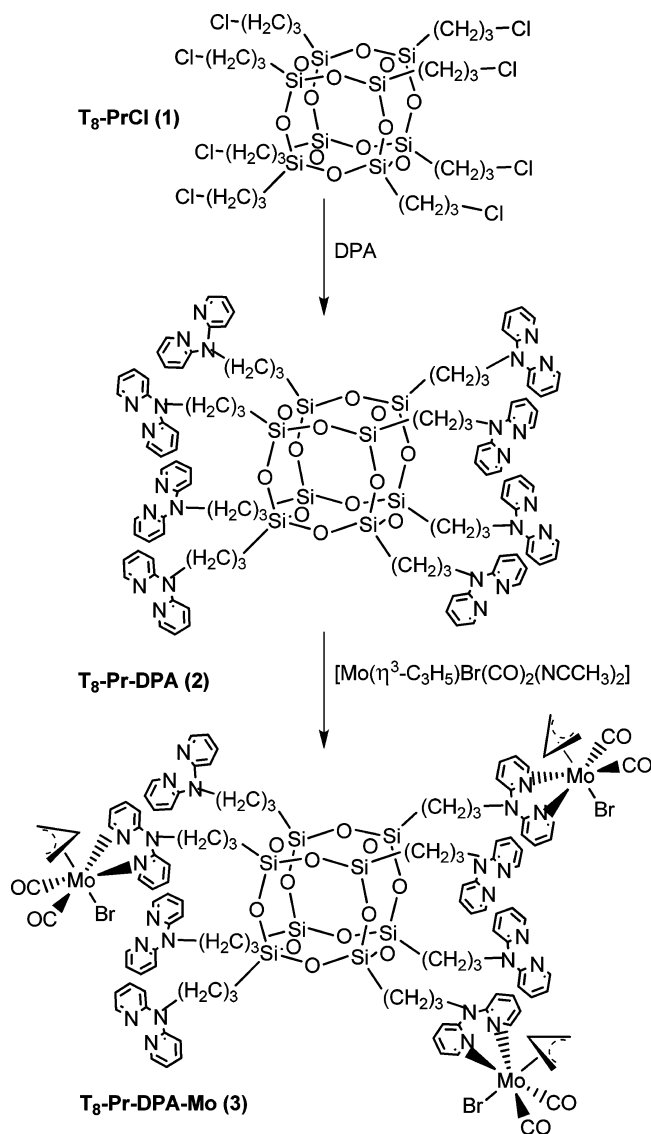
Elemental analysis was of major importance in characterizing the new nanomolecules **2** and **3**, in order to find out the extent of each reaction. **2** ( $\text{T}_8\text{-Pr-DPA}$ ) was obtained in 74% yield, and the analysis showed that the eight pendant arms in the parent silsesquioxane **1** had reacted with DPA. The final species **3** ( $\text{T}_8\text{-Pr-DPA-Mo}$ ) contained 8.06% of molybdenum. This value, as well as the corresponding ones for C, H, and N, suggests that three molybdenum units are bound to the ligand **2**. The procedure is shown in Scheme 2.

The FTIR spectrum of  $\text{T}_8\text{-PrCl}$  (**1**) exhibits the characteristic vibrational modes of the POSS cage, namely asymmetric  $\nu_{\text{Si-O-Si}}$  modes centered at  $1110\text{ cm}^{-1}$  and deformation of the Si–O–Si bridges at  $696\text{ cm}^{-1}$  (Figure 1). The presence of the propyl chain is shown by  $\nu_{\text{C-H}}$  modes at  $2994$  and  $2955\text{ cm}^{-1}$ , as well as  $\beta_{\text{C-H}}$  deformation modes at  $1458$ ,  $1436$ , and  $1410\text{ cm}^{-1}$ . The  $\nu_{\text{C-Cl}}$  stretching mode is observed at  $812\text{ cm}^{-1}$ .

In the FTIR spectrum of the new material  $\text{T}_8\text{-Pr-DPA}$  (**2**) obtained after reaction with DPA, the  $\nu_{\text{C=N}}$  modes of the pyridine rings are observed at  $1681$ ,  $1617$ , and  $1591\text{ cm}^{-1}$  and the  $\nu_{\text{C-N}}$  modes as two sharp bands at  $1316$  and  $1352\text{ cm}^{-1}$ , while the typical bands of the aromatic C–H groups appear at  $3052$ ,  $3179$ , and  $3253\text{ cm}^{-1}$  and those of aliphatic  $\text{CH}_2$  at  $2868$  and  $2943\text{ cm}^{-1}$ , with a  $\beta_{\text{C-H}}$  deformation mode at  $1440\text{ cm}^{-1}$ . The bands characteristic of the POSS cage are slightly shifted from their values in the initial compound **1** ( $\nu_{\text{Si-O-Si}}$  at  $1027$  and  $989\text{ cm}^{-1}$ , Si–O–Si deformation at  $760\text{ cm}^{-1}$ ).

Changes are detected upon the coordination of **2** to the metal fragments. The  $\nu_{\text{C=O}}$  stretching vibrations appear as very intense absorptions at  $1927$  and  $1844\text{ cm}^{-1}$ , reflecting the coordination of the  $\text{Mo}(\text{CO})_2$  fragment to the POSS. These modes were observed at  $1929$  and  $1840\text{ cm}^{-1}$  in the parent complex. The positions of  $\nu_{\text{C=N}}$  modes of the DPA ligand have changed to  $1635$  and  $1583\text{ cm}^{-1}$  and the aromatic  $\nu_{\text{C-H}}$  modes

Scheme 2



to 3282, 3235, 3195, and 3134  $\text{cm}^{-1}$ . These values are also the same as in the mononuclear complex  $[\text{Mo}(\eta^3\text{-C}_3\text{H}_5)\text{Br}(\text{CO})_2(\text{DPA})]$ .<sup>30</sup>

The modes assigned to the groups in the propyl chains are slightly different, as shown by the  $\beta_{\text{C-H}}$  band at 1478  $\text{cm}^{-1}$  and the  $\nu_{\text{C-H}}$  bands at 2998 and 2934  $\text{cm}^{-1}$ . The identity of the silsesquioxane cage is indicated by the  $\nu_{\text{Si-O-Si}}$  bands at 1062, 1023, and 1011  $\text{cm}^{-1}$  and the deformation of the Si-O-Si bridges at 769  $\text{cm}^{-1}$ .

The  $^1\text{H}$  NMR spectrum of  $T_8\text{-PrCl (1)}$  shows three signals (Figure 2) of the propyl chain protons at 0.80 (Si-CH<sub>2</sub>), 1.88 (-CH<sub>2</sub>-) and 3.54 ppm ( $\text{H}_2\text{C-Cl}$ ), while the corresponding carbon signals are observed in the  $^{13}\text{C}$  NMR spectrum at 9.6, 26.6, and 47.4 ppm.

The three proton signals are shifted to 0.85 (Si-CH<sub>2</sub>), 1.83 (-CH<sub>2</sub>-), and 2.92 ppm ( $\text{H}_2\text{C-N}$ ) in  $T_8\text{-Pr-DPA (2)}$ , the maximum deviation being observed for the proton now next to nitrogen. Similar effects are observed in the  $^{13}\text{C}$  NMR spectra, with the carbon atoms CH<sub>2</sub>-Si, CH<sub>2</sub>-CH<sub>2</sub>Si, and CH<sub>2</sub>-N appearing at 14.4, 23.0, and 63.5 ppm, respectively. The signals at 112.2, 116.8, 138.4, 148.0, and 154.5 ppm are assigned to the

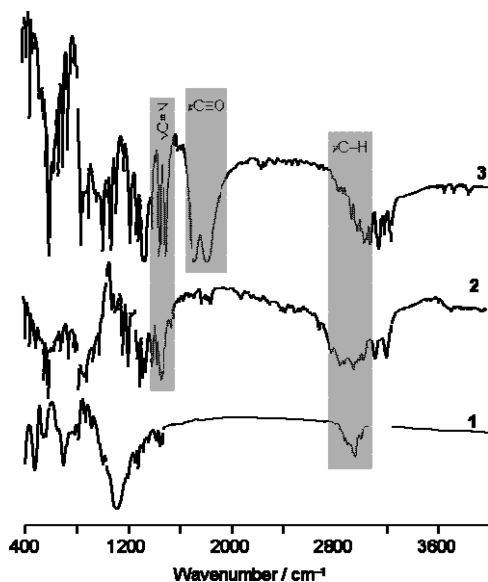


Figure 1. FTIR spectra of  $T_8\text{-PrCl (1)}$ ,  $T_8\text{-Pr-DPA (2)}$ , and  $T_8\text{-Pr-DPA-Mo (3)}$ .

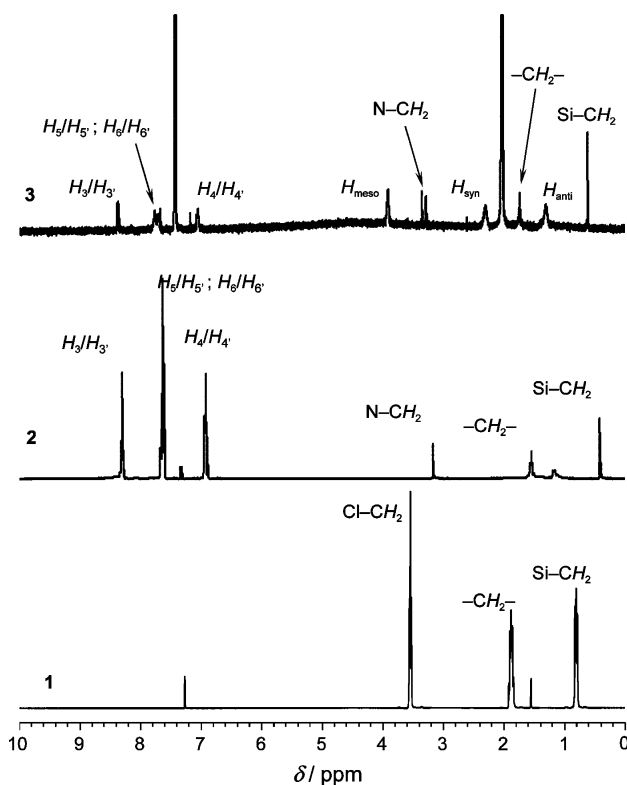


Figure 2.  $^1\text{H}$  NMR spectra of  $T_8\text{-PrCl (1)}$ ,  $T_8\text{-Pr-DPA (2)}$ , and  $T_8\text{-Pr-DPA-Mo (3)}$ .

$\text{C}_6/\text{C}_6'$ ,  $\text{C}_4/\text{C}_4'$ ,  $\text{C}_5/\text{C}_5'$ ,  $\text{C}_3/\text{C}_3'$ , and  $\text{C}_1/\text{C}_1'$  carbon atoms of DPA.

The binding of the metal fragments leads to very small shifts of the propyl chain proton signals (0.78, 1.84, and 2.95 ppm, respectively, for Si-CH<sub>2</sub>, -CH<sub>2</sub>-, and CH<sub>2</sub>-N) and those of DPA (broad singlet at 6.87 ppm,  $\text{H}_4/\text{H}_4'$ ; broad doublet at 7.55–7.63 ppm,  $\text{H}_5/\text{H}_5'$ ,  $\text{H}_6/\text{H}_6'$ ; doublet at 8.26 ppm,  $\text{H}_3/\text{H}_3'$ ). Several signals are observed for the allyl ligands, indicating the presence of several isomers, the major components appearing at 1.22, 2.85, and 3.55 ppm for  $\text{H}_{\text{anti}}$ ,  $\text{H}_{\text{syn}}$ , and  $\text{H}_{\text{meso}}$ , respectively.

The  $^{13}\text{C}$  NMR spectrum shows two signals for two of the carbon atoms of the propyl chain, namely at 31.2 and 32.3 ppm for  $-\text{CH}_2-$  and at 61.5 and 72.0 ppm for  $\text{H}_2\text{C}-\text{N}$ , significantly shifted from those of species **2** before binding of the metal. The third C atom, assigned to the peak at 15.4 ppm ( $\text{CH}_2-\text{Si}$ ), is further away from the DPA and the deviation is smaller. The signals of the carbon atoms of DPA are seen at 118.1 ( $\text{C}_6/\text{C}_6'$ ), 118.7 ( $\text{C}_4/\text{C}_4'$ ), 137.4 ( $\text{C}_5/\text{C}_5'$ ), 151.9 ( $\text{C}_3/\text{C}_3'$ ), and 163.8 ppm ( $\text{C}_1/\text{C}_1'$ ).

The  $^{29}\text{Si}$  NMR spectrum of  $\text{T}_8\text{-PrCl}$  (**1**) shows a signal at  $\delta$   $-67.0$  ppm (Figure 3), which appears in the range observed for

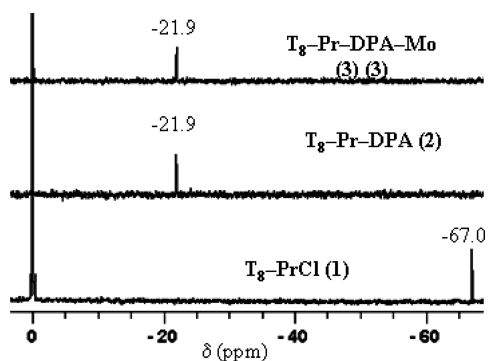


**Figure 3.**  $^{29}\text{Si}$  NMR spectra of  $\text{T}_8\text{-PrCl}$  (**1**),  $\text{T}_8\text{-Pr-DPA}$  (**2**), and  $\text{T}_8\text{-Pr-DPA-Mo}$  (**3**).

the same compound by other authors ( $-66.2$  to  $-68.0$  ppm) and is typical of a  $\text{T}^3$  species ( $\text{T}^m = \text{RSi}(\text{OSi})_m(\text{OR}')_{3-m}$ ).<sup>3</sup> In the  $^{29}\text{Si}$  spectrum of  $\text{T}_8\text{-Pr-DPA}$  (**2**), a single resonance has been observed at  $-21.9$  ppm, which confirms that all the Cl substituents have been replaced by DPA groups, leading to a considerable change in the environment. This value is lower than all those reported in a recent review of POSS derivatives, reflecting the nature of the DPA group.<sup>3</sup> However, a single resonance was also observed for  $\text{T}_8\text{-Pr-DPA-Mo}$  (**3**) having the same chemical shift as in **2**. This fact shows that coordination of molybdenum to DPA does not influence significantly the chemical environment of the POSS derivative. No conclusions can therefore be drawn regarding the number of molybdenum fragments bound to the POSS cage.

DFT calculations<sup>33</sup> (see Computational Details) were performed for  $\text{T}_8\text{-PrCl}$  (**1**) and for models of the substituted POSS with one DPA group (**2'**) and with one pendant Mo complex (**3'** and **3''**, see Figure S1 in the Supporting Information) aiming at a better understanding of the  $^{29}\text{Si}$  NMR results, presented above. In all cases the same mean Si chemical shift was obtained from the calculations ( $-74$  ppm) with a maximum deviation of 3 ppm for all Si atoms in the various solids. The chemical shift calculated for **1** agrees well with the experimental value (within 7 ppm), but the difference observed in the experimental spectra of the substituted solid is not reproduced by the calculations, most probably owing to the simplicity of the monosubstituted models employed in the calculations.

Despite the limitations of the DFT calculations, they can be used to assess the influence of Mo on the Si chemical shift. In fact, the values calculated for the Si atoms of the substituted arms in models **2'** and **3'** are within 1.5 ppm, indicating that both one DPA group and one Mo complex have similar influences on the neighboring Si atom, in good agreement with

the experimental  $^{29}\text{Si}$  NMR spectra that show equal chemical shifts for **2** and **3**.

The calculated  $^{13}\text{C}$  NMR chemical shifts for carbon atom next to the nitrogen ( $\text{CH}_2-\text{N}$ ) in **2'** and **3'** show an increase of about 10 ppm on going from the DPA model (**2'**,  $\delta_{\text{C}}$  49 ppm) to the model with the Mo complex (**3'**,  $\delta_{\text{C}}$  67 ppm), in good agreement with the trend verified experimentally.

Compound **3** was also examined by  $^{95}\text{Mo}$  NMR spectroscopy, as were the free complex  $[\text{Mo}(\eta^3\text{-C}_3\text{H}_5)(\text{CO})_2\text{Br}(\text{DPA})]$  and its precursor  $[\text{Mo}(\eta^3\text{-C}_3\text{H}_5)(\text{CO})_2\text{Br}(\text{NCMe})_2]$  for comparison. Despite the low solubility of the compounds, their  $^{95}\text{Mo}$  NMR spectra, displayed in Figure 4, show three to

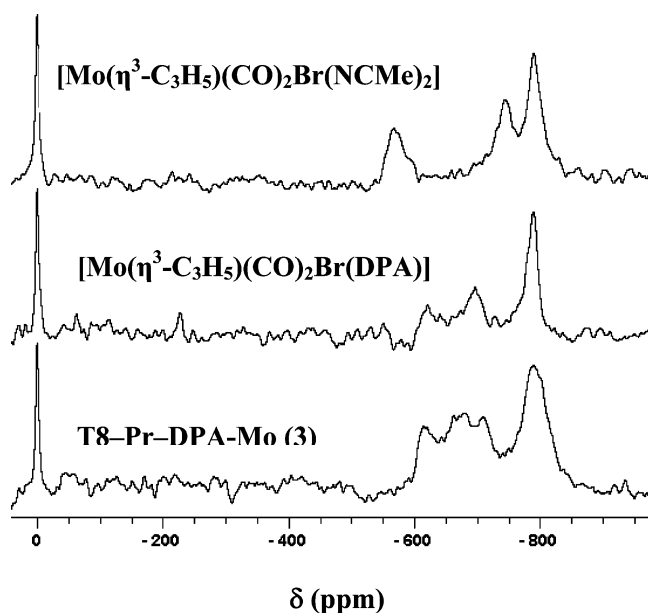


**Figure 4.**  $^{95}\text{Mo}$  NMR spectra of  $\text{T}_8\text{-Pr-DPA-Mo}$  (**3**),  $[\text{Mo}(\eta^3\text{-C}_3\text{H}_5)(\text{CO})_2\text{Br}(\text{DPA})]$ , and  $[\text{Mo}(\eta^3\text{-C}_3\text{H}_5)(\text{CO})_2\text{Br}(\text{NCMe})_2]$ .

four resonances, which can be explained by the coexistence of several isomers in solution, usually detected in  $[\text{Mo}(\eta^3\text{-C}_3\text{H}_5)(\text{CO})_2\text{LLX}]$  derivatives.<sup>29,30</sup> This observation is also supported by published studies which indicate that  $^{95}\text{Mo}$  NMR is sensitive to minor variations about the Mo center as a result of subtle electronic and steric effects.<sup>34,35</sup> The range in observed chemical shifts is  $-567$  to  $-790$  ppm with respect to  $\text{Na}_2\text{MoO}_4$  (all values are available in Table S1 in the Supporting Information). Although no reference to  $^{95}\text{Mo}$  chemical shifts of similar compounds was found in the literature, the observed resonances lie around the central portion of the usual chemical shift range for monomeric  $\text{Mo}(\text{II})$  complexes.<sup>34</sup> The main isomer of the complex  $[\text{Mo}(\eta^3\text{-C}_3\text{H}_5)(\text{CO})_2\text{Br}(\text{DPA})]$  in solution, as previously determined by  $^1\text{H}$  NMR spectroscopy,<sup>30</sup> corresponds to the exo conformation of the equatorial isomer (see Scheme 1). Therefore, on the basis of the relative intensities found on the respective  $^{95}\text{Mo}$  NMR spectrum, the upfield resonance at  $-789$  ppm can be assigned to that isomer and the second more intense signal, at  $-696$  ppm, to the exo/axial isomer. The observation of Mo chemical shifts of exo isomers at  $\delta$  values lower than those of the corresponding endo isomers is in accordance with published results involving  $^{95}\text{Mo}$  NMR studies on  $\text{Mo}(\eta^3\text{-C}_3\text{H}_5)\text{Cp}(\text{CO})_2$  derivatives.<sup>35</sup> The spectrum of  $\text{T}_8\text{-Pr-DPA-Mo}$  (**3**) shows signals broader than those of the free complex, as expected, owing to the increase in molecular size, but no significant differences are apparent in the

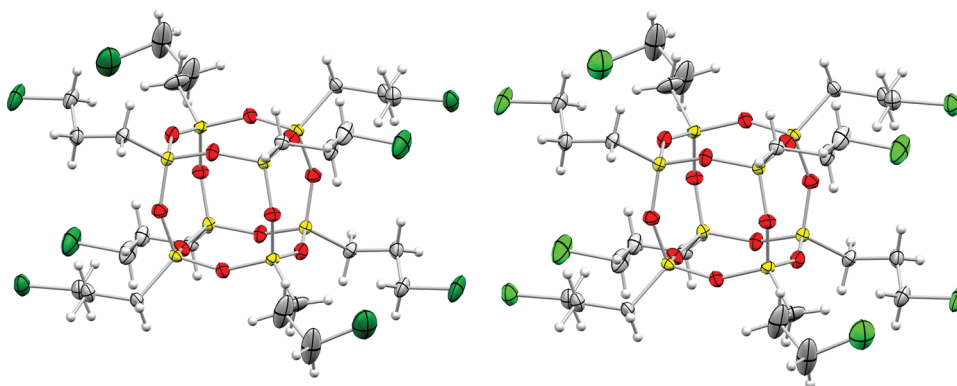


**Figure 5.** Molecular structure of  $T_8$ -PrCl (**1**) with silicon atoms in yellow, carbon in gray, oxygen in red, chlorine in green, and hydrogen in white. The disordered chain is presented only in one position for clarity. Thermal ellipsoids are drawn at the 50% probability level.

Mo chemical shift range of those two compounds, both presenting the more shielded signal at  $-789$  ppm (also very close to the corresponding signal in the precursor,  $[\text{Mo}(\eta^3\text{-C}_3\text{H}_5)(\text{CO})_2\text{Br}(\text{NCMe})_2]$ , found at  $\delta -790$  ppm).

These results show that the molybdenum chemical shift is insensitive to the presence of the cage (**3** compared to  $[\text{Mo}(\eta^3\text{-C}_3\text{H}_5)(\text{CO})_2\text{Br}(\text{DPA})]$ ) and also to the nature of the nitrogen ligand (DPA or two acetonitriles) and is characteristic of the metal formal oxidation state.

Interestingly, the  $^{95}\text{Mo}$  NMR chemical shifts calculated by DFT for the solids substituted with one Mo complex agree very well with the experimental trend discussed above. The Mo chemical shift obtained for the model with an exo coordination of the allyl ligand (**3'**) is 257 ppm below the corresponding shift in the model with an endo coordination of allyl (**3''**) and, in addition, **3'** is more stable than **3''** by 7 kcal mol $^{-1}$ , indicating that the exo isomer should be the dominant one in solution.

Suitable crystals for X-ray diffraction studies were grown by diffusion of ether into a methanol solution of  $T_8$ -PrCl (**1**). In the crystal structure, there are two independent molecules, both exhibiting crystallographic inversion symmetry and one chloropropyl chain disordered over two positions. Furthermore, they have identical distances and angles. The molecular structure of one of these molecules, presented in Figure 5, shows a POSS cubic core composed of eight tetrahedral silicon centers bridged by oxygen atoms with Si–O distances ranging from 1.616(2) to 1.631(2) Å. The Si–C distances vary between 1.836(2) and 1.858(2) Å. The crystal structure of another polymorph of this compound was recently reported at room temperature.<sup>32</sup> This polymorph also crystallizes in the triclinic space group  $P\bar{1}$ , but the unit cell contains only one independent molecule with a centrosymmetric structure. Therefore, the structure reported here, measured at 150 K, corresponds to a new polymorph, which corroborates that **1** undergoes a phase change to another triclinic structure at low temperature as suggested earlier.<sup>32</sup> Indeed, the cell parameters,  $a = 10.2067(6)$  Å,  $b = 15.2037(9)$  Å, and  $c = 15.5094(9)$  Å, differ significantly from those determined in the high-temperature polymorph ( $a = 10.020(1)$  Å,  $b = 10.133(1)$  Å, and  $c = 12.855(1)$  Å). The distances and angles within the POSS structure are identical in both polymorphs.

The X-ray single-crystal structure determination of the related  $\text{Cl}_8\text{Si}_8\text{O}_{12}$  revealed a structure with  $\bar{3}$  crystallographic symmetry and three independent Si–O distances of 1.595(4), 1.605(4), and 1.610(4) Å,<sup>36</sup> which are slightly shorter than in  $T_8$ -PrCl (**1**). A trend toward slightly narrower O–Si–O angles

( $148.8(3)$  and  $148.0(3)^\circ$ ) is also observed, while the Si–O–Si angles in **1** spread over a wider range ( $\sim 146.6(1)$  to  $\sim 151.8(1)^\circ$ ). The substitution of  $-\text{Cl}$  by  $-(\text{CH}_2)_3\text{Cl}$  results in an expansion of the cage that is more evident when the Si...Si diagonal distances measured respectively along the body ( $\text{Si}_{\text{bd}}\cdots\text{Si}_{\text{bd}}$ ) and the faces of the cube ( $\text{Si}_{\text{fc}}\cdots\text{Si}_{\text{fc}}$ ) are compared. In the chloride analogue the  $\text{Si}_{\text{bd}}\cdots\text{Si}_{\text{bd}}$  distances are 5.359(8) and 5.331(5) Å and the  $\text{Si}_{\text{fc}}\cdots\text{Si}_{\text{fc}}$  distances are 3.657(7) and 3.735(7) Å, whereas the two independent molecules of **1** have longer Si...Si distances, in particular  $\text{Si}_{\text{fc}}\cdots\text{Si}_{\text{fc}}$  distances ranging from 4.359(1) to 4.444(1)(9) Å. The  $\text{Si}_{\text{bd}}\cdots\text{Si}_{\text{bd}}$  distances vary between 5.384(1) and 5.450(1) Å.

The three compounds were also characterized by X-ray powder diffraction, which showed the modification of the diffraction patterns illustrating the change of phase and the clear loss of crystallinity (Figure S2 in the Supporting Information).

The activity of the Mo-derivatized silsesquioxane  $T_8$ -Pr-DPA-Mo (**3**) as a catalyst precursor for the epoxidation of olefins was investigated for cyclooctene (Cy8) and styrene (Sty), with *tert*-butyl hydroperoxide (TBHP) as the oxygen source, at 328 K in air with 3 mL of dichloromethane as solvent (Figure S3 (Supporting Information) and Table 1). Gas chromatography

**Table 1.** Conversions and Turnover Frequencies (TOF) for Epoxidation of Cyclooctene and Styrene Promoted by  $T_8$ -Pr-DPA-Mo (**3**) and  $[\text{Mo}(\eta^3\text{-C}_3\text{H}_5)\text{Br}(\text{CO})_2(\text{DPA})]$  in the Presence of TBHP

cat. precursor	substrate	conversion <sup>a</sup> (%)	TOF <sup>b</sup>
$T_8$ -Pr-DPA-Mo ( <b>3</b> )	Cy8	59	129
	Sty	36	80
$[\text{Mo}(\eta^3\text{-C}_3\text{H}_5)\text{Br}(\text{CO})_2(\text{DPA})]$	Cy8	70	63
	Sty	43	116

<sup>a</sup>Conversion at 24 h. <sup>b</sup>In units of mol (mol of Mo) $^{-1}$  h $^{-1}$ .

coupled to mass spectrometry (GC-MS) analysis was performed to monitor the catalytic epoxidation. The same study was performed using the complex  $[\text{Mo}(\eta^3\text{-C}_3\text{H}_5)\text{Br}(\text{CO})_2(\text{DPA})]$ ,<sup>30</sup> in order to compare the mononuclear species under the same conditions, with the nanomolecular species **3**.

Both the material  $T_8$ -Pr-DPA-Mo (**3**) and the complex  $[\text{Mo}(\eta^3\text{-C}_3\text{H}_5)\text{Br}(\text{CO})_2(\text{DPA})]$  catalyzed selectively the oxidation of the two substrates to the corresponding epoxides, without formation of diols. The results for the complex were reported previously<sup>30</sup> and follow the described activity of the

family of  $[\text{Mo}(\eta^3\text{-allyl})\text{X}(\text{CO})_2(\text{N}-\text{N})]$  complexes with  $\text{X} = \text{Cl}, \text{Br}$ , allyl =  $\text{C}_3\text{H}_5, \text{C}_5\text{H}_5\text{O}$ , and  $\text{N}-\text{N} =$  bidentate nitrogen ligand,<sup>37</sup> although the DPA ligand does not lead to a very efficient catalyst. This complex immobilized in two different types of clays (PILC and PCH) also exhibited a similar (low) activity. The total conversions are very modest compared to others obtained when the catalytic precursors were analogous Mo(II) systems bearing different nitrogen ligands, used either under homogeneous conditions<sup>37</sup> or after being immobilized in MCM-41.<sup>38</sup> For instance, even the  $[\text{Mo}(\eta^3\text{-C}_3\text{H}_5)\text{Br}(\text{CO})_2(\text{NCCH}_3)_2]$  precursor exhibited a TOF of 222 mol (mol of Mo)<sup>-1</sup> h<sup>-1</sup> and 100% conversion at 24 h (Cy8).<sup>37</sup>

The results given in Table 1 (and Figure S3) show that both systems achieve similar catalytic conversions in the oxidation of cyclooctene and styrene; however, the initial activity of 129 mol (mol of Mo)<sup>-1</sup> h<sup>-1</sup> (TOF) of  $\text{T}_8\text{-Pr-DPA-Mo}$  (3) in the epoxidation of Cy8 exceeds that of  $[\text{Mo}(\eta^3\text{-C}_3\text{H}_5)\text{Br}(\text{CO})_2(\text{DPA})]$  (63 mol (mol of Mo)<sup>-1</sup> h<sup>-1</sup>). The TOF for oxidation of styrene is higher for the complex than for 3 (116 vs 80 mol (mol of Mo)<sup>-1</sup> h<sup>-1</sup>). This kind of inversion in the TOF of Cy8 (higher) and Sty (lower) after immobilization has been observed before in the catalytic epoxidation of these substrates with related homogeneous and MCM41-supported catalysts bearing other diimines. A possible explanation may arise from the fact that epoxidation of Cy8 and Sty requires different acid–base properties of the catalyst.<sup>39</sup>

The coordination of a Mo(II) complex to the POSS cage to form the organometallic species  $\text{T}_8\text{-Pr-DPA-Mo}$  (3) did not improve the properties of the catalyst precursors. On the other hand, the selectivity toward the epoxide, as confirmed by mass spectrometry, has remained as high as in the other systems investigated.

## CONCLUSIONS

All chloropropyl side chains in the POSS cage compound 1 ( $\text{T}_8\text{-PrCl}$ ) reacted with DPA, affording a new species (2,  $\text{T}_8\text{-Pr-DPA}$ ) with eight DPA arms. Further reaction with the Mo(II) complex  $[\text{Mo}(\eta^3\text{-C}_3\text{H}_5)\text{Br}(\text{CO})_2(\text{NCMe})_2]$  afforded the new derivative 3 ( $\text{T}_8\text{-Pr-DPA-Mo}$ ), which most likely contains three molybdenum atoms per cage. NMR spectroscopy of <sup>1</sup>H and <sup>29</sup>Si showed that the chemical shifts of the protons in the propyl chain changed when DPA was introduced but were insensitive to the binding to molybdenum, the same happening to the signals of the Si in the cage, a fact which was confirmed by DFT calculations. A change in the <sup>13</sup>C chemical shifts (propyl chain) was observed upon introduction of the metal, but the low quality of the spectrum could not be improved upon because of low solubility. These are, to our knowledge, the first POSS cages functionalized with eight DPA, to build a large ligand, and with DPA and three  $[\text{Mo}(\eta^3\text{-C}_3\text{H}_5)\text{Br}(\text{CO})_2(\text{DPA})]$  molecules to build a large species behaving as a small model of a heterogeneous catalyst. The precursor 1 was structurally characterized by single-crystal X-ray diffraction and shown to be the low-temperature polymorph of a recently reported compound,<sup>32</sup> differing in the packing and the size of the unit cell.

Since the family of  $[\text{Mo}(\eta^3\text{-C}_3\text{H}_5)\text{Br}(\text{CO})_2(\text{N})_2]$  complexes has been shown to promote efficiently the catalytic epoxidation of olefins in the presence of TBHP, the activities of 3 ( $\text{T}_8\text{-Pr-DPA-Mo}$ ) and the related DPA complex (already known)<sup>30</sup> were compared.  $[\text{Mo}(\eta^3\text{-C}_3\text{H}_5)\text{Br}(\text{CO})_2(\text{DPA})]$  is not among the most active of the possible precursors, but there is no visible cooperative effect induced by the presence of several Mo atoms

in the same nanomolecule, the conversion and TOF for both cyclooctene and styrene remaining relatively small in 3.

## EXPERIMENTAL SECTION

**General Procedures.** All reagents were obtained from Aldrich and used as received. Commercial grade solvents were dried and deoxygenated by standard procedures (Et<sub>2</sub>O, THF, and toluene over Na/benzophenone ketyl; CH<sub>2</sub>Cl<sub>2</sub> over CaH<sub>2</sub>), distilled under nitrogen, and kept over 4 Å molecular sieves. The complexes  $[\text{Mo}(\eta^3\text{-C}_3\text{H}_5)\text{Br}(\text{CO})_2(\text{NCCH}_3)_2]$ <sup>29a</sup> and  $[\text{Mo}(\eta^3\text{-C}_3\text{H}_5)\text{Br}(\text{CO})_2(\text{DPA})]$ <sup>30</sup> were prepared according to literature procedures.

FTIR spectra were obtained as KBr pellets and diffuse reflectance measurements (DRIFT) using 2 cm<sup>-1</sup> resolution on a Nicolet 6700 instrument in the 400–4000 cm<sup>-1</sup> range. Powder XRD measurements were taken on a Philips PW1710 instrument using Cu K $\alpha$  radiation filtered by graphite. <sup>1</sup>H and <sup>13</sup>C solution NMR spectra were obtained with a Bruker Avance 400 spectrometer. Chemical shifts are quoted in ppm from TMS.

<sup>29</sup>Si NMR spectra in CDCl<sub>3</sub> were recorded on a Bruker Avance 400 spectrometer at 79.49 MHz with a 10 mm broad-band probe. Silicon resonances were referenced to internal standard TMS. A pulse sequence with inverse gated decoupling (waltz-16 decoupling applied during acquisition time only) was used, since the magnetogyric ratio for <sup>29</sup>Si is negative and NOE might suppress the signal. The <sup>29</sup>Si spectrum of  $\text{T}_8\text{-PrCl}$  (1) in CDCl<sub>3</sub> was obtained using the following parameters: 31.8 kHz (400 ppm) sweep width, 1.0 s acquisition time, 27  $\mu\text{s}$  (90°) pulse width, 5 s relaxation delay, 64 k data points. The <sup>29</sup>Si spectra of compounds  $\text{T}_8\text{-Pr-DPA}$  (2) and  $\text{T}_8\text{-Pr-DPA-Mo}$  (3), less soluble than 1, were obtained using a DEPT sequence optimized for coupling with two protons (DEPT 45) and a coupling constant of 7 Hz.

<sup>95</sup>Mo NMR spectra were recorded on a Bruker Avance 400 spectrometer with a 10 mm broad-band probe at 26.05 MHz; a version of the antiacoustic ringing pulse sequence (from the Bruker library) was used in order to reduce baseline distortions. Saturated solutions of the samples in DMSO-*d*<sub>6</sub> were measured at 303 K and the chemical shifts referenced to 2 M Na<sub>2</sub>MoO<sub>4</sub> in D<sub>2</sub>O (pH 11) as the external standard. The pulse parameters were as follows: 57.5 kHz sweep width, 31  $\mu\text{s}$  (90°) pulse width, 0.14 s acquisition time, 0.01 to 1 s relaxation delay, 16 k data points. Zero filling to 32 k and an exponential window function was applied with a line broadening of 150 Hz before Fourier transform to obtain a reasonable signal to noise (S/N) ratio. Topspin3 software from Bruker was used for data processing.

Microanalyses (C, N, H) were performed at the University of Vigo, and atomic absorption for determination of molybdenum was performed on a Unicam 929AA spectrometer at the Departamento de Química e Bioquímica, Faculdade de Ciências da Universidade de Lisboa.

**Synthesis of Octakis(3-chloropropyl)octasilsesquioxane (1,  $\text{T}_8\text{-PrCl}$ ).** 3-Chloropropyltriethoxysilane (225 mL) was added to a stirred mixture of methanol (4 L) and concentrated hydrochloric acid (35 mL) under a slow continuous nitrogen purge. The reaction mixture was stirred for 6 weeks. The resultant solution was then filtered and dried to give a white solid in 35% yield.

Anal. Calcd for Si<sub>8</sub>O<sub>12</sub>C<sub>24</sub>H<sub>48</sub>Cl<sub>8</sub> (1036.9): C, 27.80; H, 4.67. Found: C, 27.94; H, 4.93. IR (KBr;  $\nu$ , cm<sup>-1</sup>): 2994 (m), 2955 (m), 1193 (vs), 1111 (s). <sup>1</sup>H NMR (400.13 MHz, CDCl<sub>3</sub>, 298 K;  $\delta$ , ppm): 0.80 (t, 2H, H<sub>1</sub>), 1.88 (t, 2H, H<sub>2</sub>), 3.54 (t, 2H, H<sub>3</sub>). <sup>13</sup>C{<sup>1</sup>H} NMR (100.61 MHz, CDCl<sub>3</sub>, 298 K;  $\delta$ , ppm): 9.64 (C<sub>1</sub>), 26.55 (C<sub>2</sub>), 47.35 (C<sub>3</sub>). <sup>29</sup>Si{<sup>1</sup>H} NMR (79.49 MHz, CDCl<sub>3</sub>, 298 K;  $\delta$ , ppm): -66.97.

**Octakis[3-(2,2'-dipyridylamine)propyl]octasilsesquioxane (2,  $\text{T}_8\text{-Pr-DPA}$ ).** A solution of 2,2'-dipyridylamine (1.310 g, 7.7 mmol) in anhydrous dimethylformamide (10 mL) was added via an addition funnel, over a period of 30 min, to a stirred suspension of sodium hydride (60% dispersion in mineral oil; 0.308 g, 7.7 mmol) in anhydrous dimethylformamide (10 mL), at 0 °C under nitrogen. The mixture was stirred continuously for 2 h at that temperature.  $\text{T}_8\text{-PrCl}$  (1; 1.0 g, 0.96 mmol) and 10 mL of anhydrous dimethylformamide

were then added to the reaction mixture. The temperature was raised to room temperature, and stirring was continued for 22 h to afford a pale yellow solution. Distilled water was then added, and the desired product was extracted with chloroform. The resulting solution was dried over anhydrous sodium sulfate, filtered, and evaporated to dryness under vacuum to give the modified silsesquioxane T<sub>8</sub>-Pr-DPA in 74% yield (1.5 g).

Anal. Calcd for Si<sub>8</sub>O<sub>12</sub>C<sub>104</sub>H<sub>112</sub>N<sub>24</sub> (2114.8): C, 59.06; N, 15.90; H, 5.34. Found: C, 59.18; N, 15.56; H, 5.90. IR (KBr;  $\nu$ , cm<sup>-1</sup>): 3255 (m), 3179 (m), 3025 (s), 2846 (m), 1681 (w), 1617 (s), 1591 (s), 1440 (vs), 1352 (s), 1316 (m), 1055 (vs), 1027 (vs), 989 (vs), 760 (s). <sup>1</sup>H NMR (400.13 MHz, CDCl<sub>3</sub>, 298 K;  $\delta$ , ppm): 0.85 (t, 16H, H<sub>9</sub>), 1.23 (s, 16H, H<sub>8</sub>), 2.92 (s, 16H, H<sub>7</sub>), 6.80 (t, 16H, H<sub>4</sub>/H<sub>4</sub>'), 7.56 (m, 32H, H<sub>5</sub>/H<sub>5</sub>' and H<sub>6</sub>/H<sub>6</sub>'), 8.25 (d, 16H, H<sub>3</sub>/H<sub>3</sub>'). <sup>13</sup>C{<sup>1</sup>H} NMR (100.61 MHz, CDCl<sub>3</sub>, 298 K;  $\delta$ , ppm): 14.4 (C<sub>9</sub>), 23.0 (C<sub>8</sub>), 63.5 (C<sub>7</sub>), 112.2 (C<sub>6</sub>/C<sub>6</sub>'), 116.8 (C<sub>4</sub>/C<sub>4</sub>'), 138.4 (C<sub>5</sub>/C<sub>5</sub>'), 148.0 (C<sub>3</sub>/C<sub>3</sub>'), 154.5 (C<sub>1</sub>/C<sub>1</sub>'). <sup>29</sup>Si{<sup>1</sup>H} NMR (79.49 MHz, CDCl<sub>3</sub>, 298 K;  $\delta$ , ppm): -21.87.

**Octakis[3-(2,2-dipyridylamine)propyl]octasilsesquioxane-[Mo(allyl)Br(CO)<sub>2</sub>] (3, T<sub>8</sub>-Pr-DPA-Mo).** Octakis[3-(2,2-dipyridylamine)propyl]octasilsesquioxane, T<sub>8</sub>-Pr-DPA (2; 1.0 g, 0.47 mmol), was added to a stirred solution of [Mo( $\eta^3$ -C<sub>3</sub>H<sub>5</sub>)Br(CO)<sub>2</sub>(NCCCH<sub>3</sub>)<sub>2</sub>] (1.34 g, 3.8 mmol) in anhydrous ethanol (25 mL) under nitrogen, and the mixture was stirred overnight at room temperature. The solvent was removed by filtration and the solid was washed three times with anhydrous dichloromethane and dried, giving 1.3 g of T<sub>8</sub>-Pr-DPA-Mo (98% yield).

Anal. Calcd for Si<sub>8</sub>O<sub>18</sub>C<sub>119</sub>H<sub>127</sub>N<sub>24</sub>Br<sub>3</sub>Mo<sub>3</sub> (2934.3; 3 Mo units): C, 48.72; N, 11.46; H, 4.36; Mo, 9.81. Found: C, 47.34; N, 10.68; H, 4.62; Mo, 8.06. IR (KBr;  $\nu$ , cm<sup>-1</sup>): 3282 (s), 3235 (s), 3195 (s), 3134 (s), 2998 (m), 2934 (w), 1927 (vs), 1843 (vs), 1635 (s), 1594 (m), 1583 (s), 1478 (vs), 1369 (m), 1062 (s), 1023 (s), 1011 (vs), 769 (vs). <sup>1</sup>H NMR (400.13 MHz, CDCl<sub>3</sub>, 298 K;  $\delta$ , ppm): 0.78 (s bd, 16H, H<sub>9</sub>), 1.22 (s, bd, allyl), 1.84 (s bd, 16H, H<sub>8</sub>), 2.85 (s, bd, allyl), 2.95 (s bd, 16H, H<sub>7</sub>), 3.55 (s, bd, allyl), 6.87 (s bd, 16H, H<sub>4</sub>/H<sub>4</sub>'), 7.55–7.63 (d bd, 32H, H<sub>5</sub>/H<sub>5</sub>' and H<sub>6</sub>/H<sub>6</sub>'), 8.26 (d bd, 16H, H<sub>3</sub>/H<sub>3</sub>'). <sup>13</sup>C{<sup>1</sup>H} NMR (100.61 MHz, CDCl<sub>3</sub>, 298 K;  $\delta$ , ppm): 15.4 (C<sub>9</sub>), 31.2/32.3 (C<sub>8</sub>), 50.2 (allyl), 61.5/72.0 (C<sub>7</sub>), 75.1 (allyl), 118.1 (C<sub>6</sub>/C<sub>6</sub>'), 118.7 (C<sub>4</sub>/C<sub>4</sub>'), 137.4 (C<sub>5</sub>/C<sub>5</sub>'), 151.9 (C<sub>3</sub>/C<sub>3</sub>'), 163.8 (C<sub>1</sub>/C<sub>1</sub>'). <sup>29</sup>Si{<sup>1</sup>H} NMR (79.49 MHz, CDCl<sub>3</sub>, 298 K;  $\delta$ , ppm): -21.91. <sup>95</sup>Mo NMR (26.05 MHz, DMSO-*d*<sub>6</sub>, 303 K;  $\delta$ , ppm): -615, -678 (endo isomers); -709 (exo/axial); -789 (exo/equatorial).

**Crystallography.** Crystals of 1 with suitable quality for a single-crystal X-ray determination were grown from diffusion of ether into a methanol solution of 1. Crystal data: C<sub>24</sub>H<sub>48</sub>Cl<sub>8</sub>O<sub>12</sub>Si<sub>8</sub>P<sub>2</sub>, M<sub>r</sub> = 1036.94, triclinic, space group P $\bar{1}$ , Z = 2, a = 10.2067(6) Å, b = 15.2037(9) Å, c = 15.5094(9) Å,  $\alpha$  = 99.157(3)°,  $\beta$  = 103.552(3)°,  $\gamma$  = 99.353(3)°, V = 2259.3(2) Å<sup>3</sup>,  $\rho$ (calcd) = 1.524 Mg m<sup>-3</sup>,  $\mu$ (Mo K $\alpha$ ) = 0.761 mm<sup>-1</sup>, 120 818 reflections collected, 20 206 unique reflections (R<sub>int</sub> = 0.0315). The final R values were R1 = 0.0581 and wR2 = 0.1581 for 14 010 reflections with I > 2 $\sigma$ (I) and R1 = 0.0924 and wR2 = 0.1887 for all hkl data.

The X-ray data were collected on a CCD Bruker APEX II diffractometer at 150(2) K using graphite-monochromated Mo K $\alpha$  radiation ( $\lambda$  = 0.710 73 Å). The crystal was positioned at 35 mm from the CCD, and the spots were measured using a counting time of 10 s. Data reduction including a multiscan absorption correction was carried out using the SAINT-NT software from Bruker AXS. The structure was solved using SHELXS-97 and refined using full-matrix least squares in SHELXL-97.<sup>40</sup> The disordered chloropropyl chains were refined with the chlorine and the two subsequent carbon atoms occupying two alternative positions with their occupancies set to 0.5 for the first molecule, whereas for the second molecule refined occupancies of x and 1 - x, with x equal to 0.29(1), were used. Anisotropic thermal parameters were used for all non-hydrogen atoms. The C-H hydrogen atoms were included at calculated positions and refined with isotropic parameters equivalent to 1.2 times those of the atom to which they were attached. The residual electronic density was in the range +2.79 to -1.87 Å<sup>-3</sup>, with the highest positive peak 0.75 Å within the coordination sphere of a disordered chloride.

The molecular diagram presented was drawn with the Mercury 2.3 software available from CSD.<sup>41</sup>

**Catalytic Studies.** T<sub>8</sub>-Pr-DPA-Mo (3) and [Mo( $\eta^3$ -C<sub>3</sub>H<sub>5</sub>)Br(CO)<sub>2</sub>(DPA)] were tested in the epoxidation of *cis*-cyclooctene and styrene, using as oxidant *tert*-butyl hydroperoxide (TBHP). The catalytic oxidation of the two olefins was carried out at 328 K under a normal atmosphere in a reaction vessel equipped with a magnetic stirrer and a condenser. The vessel was loaded with olefin (100%), internal standard (DBE), catalyst (1%), oxidant (200%), and 3 mL of solvent. The course of the reaction was monitored by GC-MS analysis. The addition of the oxidant determines the initial time of the reaction. Samples were taken every 15 min during the first 1 h and then after 2, 4, 6, 8, and 24 h of reaction. They were diluted with dichloromethane and chilled in an ice bath. For the destruction of *tert*-butyl hydroperoxide, a catalytic amount of manganese dioxide was added. The resulting slurry was filtered and the resulting extract injected into the GC-MS system. The conversion of each olefin, measured by the formation of the corresponding epoxide, was quantified through GC-MS using convenient calibration plots recorded prior to the reaction course. Blank experiments using TBHP/MnO<sub>2</sub> and olefin were carried out, and no measurable activity was found. No reaction took place without a metal-containing catalyst.

GC-MS analysis was performed by using an Agilent 6890 Series gas chromatograph, equipped with an Agilent 7683 automatic liquid sampler and coupled to an Agilent 5973N mass selective detector (Agilent Technologies, Little Falls, DE). The GC analyses were performed on a TRB-5MS (30 m  $\times$  0.25 mm i.d.  $\times$  0.25  $\mu$ m film thickness) capillary column (5% diphenyl, 95% dimethylpolysiloxane; Teknokroma, Barcelona, Spain), and helium was used as carrier gas maintained in the constant pressure mode (7.36 psi). The oven temperature was programmed from 60 °C (held for 3 min) to 200 °C (held for 2 min) at 10 °C/min. The inlet was set at 250 °C operating with a split ratio of 25:1, and 1  $\mu$ L of each sample was injected. The transfer line, ion source, and quadrupole analyzer temperatures were maintained at 280, 230, and 150 °C, respectively, and a solvent delay of 3 min was selected. The mass selective detector operated in the full-scan mode acquisition, and electron ionization mass spectra in the range 35–550 Da were recorded at 70 eV electronic energy with an ionization current of 34.6  $\mu$ A. Data analysis and instrument control were performed by the MSD ChemStation software (G1701CA, version C.00.00; Agilent Technologies). For the determination of the conversion percentages, the ratio of the abundance areas of olefins and DBE was calculated.

**Epoxidation of *cis*-Cyclooctene:** *cis*-cyclooctene (800 mg, 7.3 mmol), 800 mg of dibutyl ether (internal standard), 1 mol % of catalyst, 2.65 mL of TBHP (5.5 M in *n*-decane), and 3 mL of CH<sub>2</sub>Cl<sub>2</sub>.

**Epoxidation of Styrene:** styrene (800 mg, 7.7 mmol), 800 mg of dibutyl ether (internal standard), 1 mol % of catalyst, 2.65 mL of TBHP (5.5 M in *n*-decane), and 3 mL of CH<sub>2</sub>Cl<sub>2</sub>.

**Computational Details.** All calculations were performed using the Gaussian 03 software package<sup>42</sup> and the B3LYP hybrid functional. That functional includes a mixture of Hartree-Fock<sup>43</sup> exchange with DFT<sup>33</sup> exchange correlation, given by Becke's three-parameter functional<sup>44</sup> with the Lee, Yang, and Parr correlation functional, which includes both local and nonlocal terms.<sup>45,46</sup> All geometry optimizations were performed without symmetry constraints using the following basis set (b1): a LanL2DZ basis set<sup>47</sup> augmented with an f polarization function<sup>48</sup> for Mo and a standard 6-31G(d,p) set<sup>49</sup> for the remaining elements. NMR shielding tensors were calculated using the gauge-independent atomic orbital method (GLAO)<sup>50</sup> with the same functional, an improved basis set (b2), and geometries optimized at the B3LYP/b1 level. Basis b2 consisted of a standard 3-21G set<sup>51</sup> with an added f polarization function<sup>47</sup> for Mo and a 6-311+G(2d,p) set<sup>52</sup> for the remaining elements. The calculations were performed for the real molecule of silsesquioxane 1 and for models of the substituted solids with only one substitution each, owing to computational limitations. The model 2' corresponds to a solid with only one DPA substituent, and models 3' and 3'' correspond to the POSS substituted with one Mo complex with the allyl ligand in the exo and in the endo conformations, respectively (see Figure S1, Supporting Information).

## ■ ASSOCIATED CONTENT

## ■ Supporting Information

<sup>95</sup>Mo NMR data (Table S1), a representation of the models used in the DFT calculations (Figure S1), X-ray powder diffraction data (Figure S2), catalytic activity (Figure S3), atomic coordinates for all optimized species, and a CIF file giving crystal data for **1**. This material is available free of charge via the Internet at <http://pubs.acs.org>.

## ■ AUTHOR INFORMATION

## Notes

The authors declare no competing financial interest.

## ■ ACKNOWLEDGMENTS

F.C.M.P. thanks the FCT for a research grant (SFRH/BD/24598/2005). L.F.V. (PTDC/QUI-QUI/099389/2008), L.F.V. and M.J.V.d.B. (PEst-OE/QUI/UI0100/2011), and M.J.C., C.D.N., P.D.V., and J.M.F.N. (PEst-OE/QUI/UI0612/2011) thank the FCT for funding. N.L.D.F. thanks FAPESP, UNESP and CAPES for scholarships.

## ■ REFERENCES

- (1) Baney, R. H.; Itoh, M.; Sabakibara, A.; Suzuki, T. *Chem. Rev.* **1995**, *95*, 1409–1430.
- (2) Quadrelli, E. A.; Basset, J.-M. *Coord. Chem. Rev.* **2010**, *254*, 707–728.
- (3) Cordes, D. B.; Lickiss, P. D.; Rataboul, F. *Chem. Rev.* **2010**, *110*, 2081–2173.
- (4) Marcolli, C.; Calzaferri, G. *Appl. Organomet. Chem.* **1999**, *13*, 213–226.
- (5) Abbenhuis, H. C. L. *Chem. Eur. J.* **2000**, *6*, 25–32.
- (6) Li, G.; Wang, L.; Ni, H.; Pittman, C. U., Jr. *J. Inorg. Organomet. Polym.* **2002**, *11*, 123–154.
- (7) Calzaferri, G.; Imhof, R.; Törnroos. *J. Chem. Soc., Dalton Trans.* **1993**, 3741–3748.
- (8) Harrison, P. G.; Kannengiesser, R. *J. Chem. Soc., Chem. Commun.* **1995**, 2065–2066.
- (9) Rattay, M.; Fenske, D.; Jutzi, P. *Organometallics* **1998**, *17*, 2930–2932.
- (10) (a) Bassindale, A. R.; Gentle, T. *J. Organomet. Chem.* **1996**, *521*, 391–393. (b) Kim, S. G.; Choi, J.; Tamaki, R.; Laine, R. M. *Polymer* **2005**, *46*, 4514–4524. (c) Braunstein, P.; Galsworthy, J. R.; Hendan, B. J.; Marsmann, H. C. *J. Organomet. Chem.* **1998**, *551*, 159–164. (d) Morán, M.; Casado, C. M.; Cuadrado, I.; Losada, J. *Organometallics* **1993**, *12*, 4327–4333.
- (11) Provas, A.; Luft, M.; Mu, J. C.; White, A. H.; Matison, J. G.; Skelton, B. W. *J. Organomet. Chem.* **1998**, *565*, 159–164.
- (12) Iacono, S. T.; Vij, A.; Grabow, W.; Smith, D. W., Jr.; Mabry, J. M. *Chem. Commun.* **2007**, 4992–4994.
- (13) Dittmar, U.; Hendan, B. J.; Flörke, U.; Marsmann, H. C. *J. Organomet. Chem.* **1995**, *489*, 185–194.
- (14) Carmo, D. R.; Paim, L. L.; Dias Filho, N. L.; Stradiotto, N. R. *Appl. Surf. Sci.* **2007**, *253*, 3683–3689.
- (15) Filho, N. L.; Dias, R. M.; Costa, R. M.; Schultz, M. S. *Inorg. Chim. Acta* **2008**, *361*, 2314–2320.
- (16) Hendan, B. J.; Marsmann, H. C. *Appl. Organomet. Chem.* **1999**, *13*, 287–294.
- (17) Cho, H. M.; Weissman, H.; Wilson, S. R.; Moore, J. S. *J. Am. Chem. Soc.* **2006**, *128*, 14742–14743.
- (18) Lucenti, E.; D'Alfonso, G.; Macchi, P.; Maranesi, M.; Roberto, D.; Sironi, A.; Ugo, R. *J. Am. Chem. Soc.* **2006**, *128*, 12054–12055.
- (19) Goodgame, D. M. L.; Kealy, S.; Lickiss, P. D.; White, A. J. P. *J. Mol. Struct.* **2008**, *890*, 232–239.
- (20) Ullah, A.; Alongi, J.; Russo, S. *Polym. Bull.* **2011**, *67*, 1169–1183.
- (21) (a) Wada, K.; Mitsudo, T.-A. *Catal. Surveys Asia* **2006**, *9*, 229–241. (b) Bent, M.; Gun'Ko, Y. *J. Organomet. Chem.* **2005**, *690*, 463–468.
- (22) Crocker, M.; Herold, R. H. M.; Orpen, A. G.; Overgaag, M. T. *A. J. Chem. Soc., Dalton Trans.* **1999**, 3791–3804.
- (23) Monticelli, O.; Cavallo, D.; Bocchini, S.; Frache, A.; Carniato, F.; Tanelotto, A. *Polym. Chem.* **2011**, *49*, 4794–4799.
- (24) Wada, K.; Itayama, N.; Watanabe, N.; Bundo, M.; Kondo, T.; Mitsudo, T.-A. *Organometallics* **2004**, *23*, 5824–5832.
- (25) Viotti, O.; Fischer, A.; Seisenbaeva, G. A.; Kessler, V. G. *Inorg. Chem. Commun.* **2010**, *13*, 774–777.
- (26) Solans-Monfort, X.; Filhol, J.-S.; Copéret, C.; Eisenstein, O. *New J. Chem.* **2006**, *30*, 842–850.
- (27) Hossain, D.; Pittman, C. U., Jr.; Hagelberg, F.; Saebo, S. *J. Phys. Chem. C* **2008**, *112*, 16070–16077.
- (28) Ahmadi, A.; McBride, C.; Freire, J. J.; Kajetanowicz, A.; Czaban, J.; Grela, K. *J. Phys. Chem. A* **2011**, *115*, 12017–12024.
- (29) (a) tom Dieck, H.; Friedel, H. *J. Organomet. Chem.* **1968**, *14*, 375–385. (b) Hayter, R. G. *J. Organomet. Chem.* **1967**, *13*, Pl–P3. (c) Baker, P. K. *Adv. Organomet. Chem.* **1996**, *40*, 45 and references therein. (d) Ascenso, J. R.; Azevedo, C. G.; Calhorda, M. J.; Carrondo, M. A. A. F. d. C. T.; Costa, P.; Dias, A. R.; Drew, M. G. B.; Galvão, A. M.; Romão, C. C.; Félix, V. *J. Organomet. Chem.* **2001**, *632*, 197–208. (e) Costa, P. M. F. J.; Mora, M.; Calhorda, M. J.; Félix, V.; Ferreira, P.; Drew, M. G. B.; Wadepohl, H. *J. Organomet. Chem.* **2003**, *687*, 57–68. (f) Martinho, P. N.; Quintal, S.; Costa, P.; Losi, S.; Félix, V.; Gimeno, M. C.; Laguna, A.; Drew, M. G. B.; Zanello, P.; Calhorda, M. J. *Eur. J. Inorg. Chem.* **2006**, 4096–4103. (g) Quintal, S.; Matos, J.; Fonseca, I.; Félix, V.; Drew, M. G. B.; Trindade, N.; Meireles, M.; Calhorda, M. J. *Inorg. Chim. Acta* **2008**, *361*, 1584–1596.
- (30) Alonso, J. C.; Neves, P.; Silva, C.; Valente, A. A.; Brandão, P.; Quintal, S.; Villa de Brito, M. J.; Pinto, P.; Félix, V.; Drew, M. G. B.; Pires, J.; Carvalho, A. P.; Calhorda, M. J.; Ferreira, P. *Eur. J. Inorg. Chem.* **2008**, 1147–1156.
- (31) Dietmar, U.; Hendan, B. J.; Flörke, U.; Marsmann, H. C. *J. Organomet. Chem.* **1995**, *489*, 185–194.
- (32) Marciniak, B.; Dutkiewicz, M.; Maciejewski, H.; Kubicki, M. *Organometallics* **2008**, *27*, 793–794.
- (33) Parr, R. G.; Yang, W. *Density Functional Theory of Atoms and Molecules*; Oxford University Press: New York, 1989.
- (34) Minelli, M.; Enemark, J. H.; Brownlee, T. C. B.; O'Connor, M. J.; Wedd, A. G. *Coord. Chem. Rev.* **1985**, *68*, 169.
- (35) Faller, J. W.; Whitmore, B. C. *Organometallics* **1986**, *5*, 752 and references therein.
- (36) Törnroos, K. W.; Calzaferri, G.; Imhof, R. *Acta Crystallogr.* **1995**, *C51*, 1732–1735.
- (37) Alonso, J. C.; Neves, P.; Pires da Silva, M. J.; Quintal, S.; Vaz, P. D.; Silva, C.; Valente, A. A.; Ferreira, P.; Calhorda, M. J.; Félix, V.; Drew, M. G. B. *Organometallics* **2007**, *26*, 5548–5556.
- (38) Vasconcellos-Dias, M.; Nunes, C. D.; Vaz, P. D.; Ferreira, P.; Brandão, P.; Félix, V.; Calhorda, M. J. *Catal.* **2008**, *256*, 301–311.
- (39) Saraiva, M. S.; Dias Filho, N. L.; Nunes, C. D.; Vaz, P. D.; Nunes, T. G.; Calhorda, M. J. *Microporous Mesoporous Mater.* **2009**, *117*, 670–677.
- (40) Sheldrick, G. M. *Acta Crystallogr.* **2008**, *A64*, 112–122.
- (41) Macrae, C. F.; Bruno, I. J.; Chisholm, J. A.; Edgington, P. R.; McCabe, P.; Pidcock, E.; Rodriguez-Monge, L.; Taylor, R.; van de Streek, J.; Wood, P. A. *J. Appl. Crystallogr.* **2008**, *41*, 466–470.
- (42) Frisch, M. J.; Trucks, G. W.; Schlegel, H. B.; Scuseria, G. E.; Robb, M. A.; Cheeseman, J. R.; Montgomery, J. A., Jr.; Vreven, T.; Kudin, K. N.; Burant, J. C.; Millam, J. M.; Iyengar, S. S.; Tomasi, J.; Barone, V.; Mennucci, B.; Cossi, M.; Scalmani, G.; Rega, N.; Petersson, G. A.; Nakatsuji, H.; Hada, M.; Ehara, M.; Toyota, K.; Fukuda, R.; Hasegawa, J.; Ishida, M.; Nakajima, T.; Honda, Y.; Kitao, O.; Nakai, H.; Klene, M.; Li, X.; Knox, J. E.; Hratchian, H. P.; Cross, J. B.; Adamo, C.; Jaramillo, J.; Gomperts, R.; Stratmann, R. E.; Yazyev, O.; Austin, A. J.; Cammi, R.; Pomelli, C.; Ochterski, J. W.; Ayala, P. Y.; Morokuma, K.; Voth, G. A.; Salvador, P.; Dannenberg, J. J.; Zakrzewski, V. G.; Dapprich, S.; Daniels, A. D.; Strain, M. C.;

Farkas, O.; Malick, D. K.; Rabuck, A. D.; Raghavachari, K.; Foresman, J. B.; Ortiz, J. V.; Cui, Q.; Baboul, A. G.; Clifford, S.; Cioslowski, J.; Stefanov, B. B.; Liu, G.; Liashenko, A.; Piskorz, P.; Komaromi, I.; Martin, R. L.; Fox, D. J.; Keith, T.; Al-Laham, M. A.; Peng, C. Y.; Nanayakkara, A.; Challacombe, M.; Gill, P. M. W.; Johnson, B.; Chen, W.; Wong, M. W.; Gonzalez, C.; Pople, J. A. *Gaussian 03, Revision C.02*; Gaussian, Inc., Wallingford, CT, 2004.

(43) Hehre, W. J.; Radom, L.; Schleyer, P. v. R.; Pople, J. A. *Ab Initio Molecular Orbital Theory*; Wiley: New York, 1986.

(44) Becke, A. D. *J. Chem. Phys.* **1993**, *98*, 5648.

(45) Miehlich, B.; Savin, A.; Stoll, H.; Preuss, H. *Chem. Phys. Lett.* **1989**, *157*, 200.

(46) Lee, C.; Yang, W.; Parr, G. *Phys. Rev. B* **1988**, *37*, 785.

(47) (a) Dunning, T. H., Jr.; Hay, P. J. In *Modern Theoretical Chemistry*; Schaefer, H. F., III, Ed.; Plenum: New York, 1976; Vol. 3, p 1. (b) Hay, P. J.; Wadt, W. R. *J. Chem. Phys.* **1985**, *82*, 270. (c) Wadt, W. R.; Hay, P. J. *J. Chem. Phys.* **1985**, *82*, 284. (d) Hay, P. J.; Wadt, W. R. *J. Chem. Phys.* **1985**, *82*, 2299.

(48) Ehlers, A. W.; Böhme, M.; Dapprich, S.; Gobbi, A.; Höllwarth, A.; Jonas, V.; Köhler, K. F.; Stegmann, R.; Veldkamp, A.; Frenking, G. *Chem. Phys. Lett.* **1993**, *208*, 111.

(49) (a) Ditchfield, R.; Hehre, W. J.; Pople, J. A. *J. Chem. Phys.* **1971**, *54*, 724. (b) Hehre, W. J.; Ditchfield, R.; Pople, J. A. *J. Chem. Phys.* **1972**, *56*, 2257. (c) Hariharan, P. C.; Pople, J. A. *Mol. Phys.* **1974**, *27*, 209. (d) Gordon, M. S. *Chem. Phys. Lett.* **1980**, *76*, 163. (e) Hariharan, P. C.; Pople, J. A. *Theor. Chim. Acta* **1973**, *28*, 213.

(50) (a) Wolinski, K.; Hilton, J. F.; Pulay, P. *J. Am. Chem. Soc.* **1990**, *112*, 8251. (b) Dodds, J. L.; McWeeny, R.; Sadlej, A. J. *Mol. Phys.* **1980**, *41*, 1419. (c) Ditchfield, R. *Mol. Phys.* **1974**, *27*, 789. (d) McWeeny, R. *Phys. Rev.* **1962**, *126*, 1028. (e) London, F. J. *Phys. Radium, Paris* **1937**, *8*, 397.

(51) (a) Binkley, J. S.; Pople, J. A.; Hehre, W. J. *J. Am. Chem. Soc.* **1980**, *102*, 939. (b) Gordon, M. S.; Binkley, J. S.; Pople, J. A.; Pietro, W. J.; Hehre, W. J. *J. Am. Chem. Soc.* **1982**, *104*, 2797. (c) Pietro, W. J.; Francl, M. M.; Hehre, W. J.; Defrees, D. J.; Pople, J. A.; Binkley, J. S. *J. Am. Chem. Soc.* **1982**, *104*, 5039. (d) Dobbs, K. D.; Hehre, W. J. *J. Comput. Chem.* **1987**, *8*, 861. (e) Dobbs, K. D.; Hehre, W. J. *J. Comput. Chem.* **1987**, *8*, 880. (f) Dobbs, K. D.; Hehre, W. J. *J. Comput. Chem.* **1986**, *7*, 359.

(52) (a) McClean, A. D.; Chandler, G. S. *J. Chem. Phys.* **1980**, *72*, 5639. (b) Krishnan, R.; Binkley, J. S.; Seeger, R.; Pople, J. A. *J. Chem. Phys.* **1980**, *72*, 650. (c) Wachters, A. J. H. *J. Chem. Phys.* **1970**, *52*, 1033. (d) Hay, P. J. *J. Chem. Phys.* **1977**, *66*, 4377. (e) Raghavachari, K.; Trucks, G. W. *J. Chem. Phys.* **1989**, *91*, 1062. (f) Binning, R. C.; Curtiss, L. A. *J. Comput. Chem.* **1990**, *11*, 1206. (g) McGrath, M. P.; Radom, L. *J. Chem. Phys.* **1991**, *94*, 511. (h) Clark, T.; Chandrasekhar, J.; Spitznagel, G. W.; Schleyer, P. v. R. *J. Comput. Chem.* **1983**, *4*, 294. (i) Frisch, M. J.; Pople, J. A.; Binkley, J. S. *J. Chem. Phys.* **1984**, *80*, 3265.